

S14-10

A quantitative analysis of the chlorophyll fluorescence induction in terms of electron transfer rates at donor and acceptor sides of photosystem II

WJ Vredenberg, GC Rodrigues, JJS van Rensen

Laboratory of Plant Physiology, Wageningen University, Arboretumlaan 4, 6703 BD Wageningen, The Netherlands. Fax +31 317 484740. E-mail: wim.vredenberg@pph.dpw.wau.nl

Keywords: photosystem II, chlorophyll a fluorescence, energy trapping, heterogeneity, electron flow rates

Introduction

The chlorophyll *a* (chl) fluorescence yield (Φ_F) of green cells and isolated chloroplasts changes upon actinic illumination. Recently the so-called three-state model of energy trapping and chlorophyll fluorescence was presented (Vredenberg, 2000) which takes into account that at least two turnovers are required for stationary closure of a reaction center (RC). An open RC is transferred with high efficiency into its semi-closed (-open) state. This state is characterized by Q_A and the primary donor of PSII (P_{680}) in the reduced state and the primary acceptor pheophytin (Phe) in the oxidized state. The fluorescence yield of a system with 100% of the centers in the semi-closed state is 50% of the maximal yield with all centers in the closed state at fluorescence level F_m . Closure of a semi-closed (-open) center requires a second turnover. The two-step closure of the RC's in a 1-s light pulse expresses itself in a poly-phasic fluorescence induction curve.

The present communication focuses on the fluorescence kinetics and multi-state transfer pattern of the reaction centers (RC) in a dark-adapted homogeneous system with the oxygen evolving complex (OEC) in a defined S-state in a 1 s light pulse. The model can easily be extended to dark-adapted systems with heterogeneity in S-states, and/or in redox state of QB. It enables quantitative analyses of the fluorescence induction curve in terms of rate constants of the light- and dark reactions at the donor and acceptor side of PSII. Examples of applications are a.o. i) donor- and/or acceptor side inhibitors, ii) atrazine resistance (van Rensen et al, these proceedings), iii) UV-B treatment (Rodrigues et al , these proceedings).

Material and Methods

Plant growth (*Chenopodium album* L. and *Solanum nigrum*) and chloroplast isolations were as described elsewhere (Vredenberg, 2000). Room temperature chlorophyll fluorescence yield was measured in dark-adapted preparation with the PEA fluorometer (PEA, Hansatech Instruments, Kings Lynn, England) during a 1-s red (maximal emission at 650 nm) light pulse of 600 W m^{-2} . The data acquisition interval was 10 μs for the first 2 ms of measurements and 1 ms thereafter. Further details about the use of this equipment can be found elsewhere (Strasser et al. 1995; Vredenberg 2000). Data analysis of experimental fluorescence curves using the set of ordinary linear differential equations (ODE) were done with Mathcad 2000 (Mathsoft Inc., Cambridge, USA) with one of its ODE solvers.

Results and Interpretation

Figure 1 shows the symbolized representation of the 18 intermediates associated with the full closure of an open reaction center in its S1-state. The transfer rate of each of the 20 states can be quantified in terms of the light excitation rate (k_L) and the rate constants of primary electron transfer between Y_Z^+ and OEC (k_{si} , $i=1,\dots,4$) and between

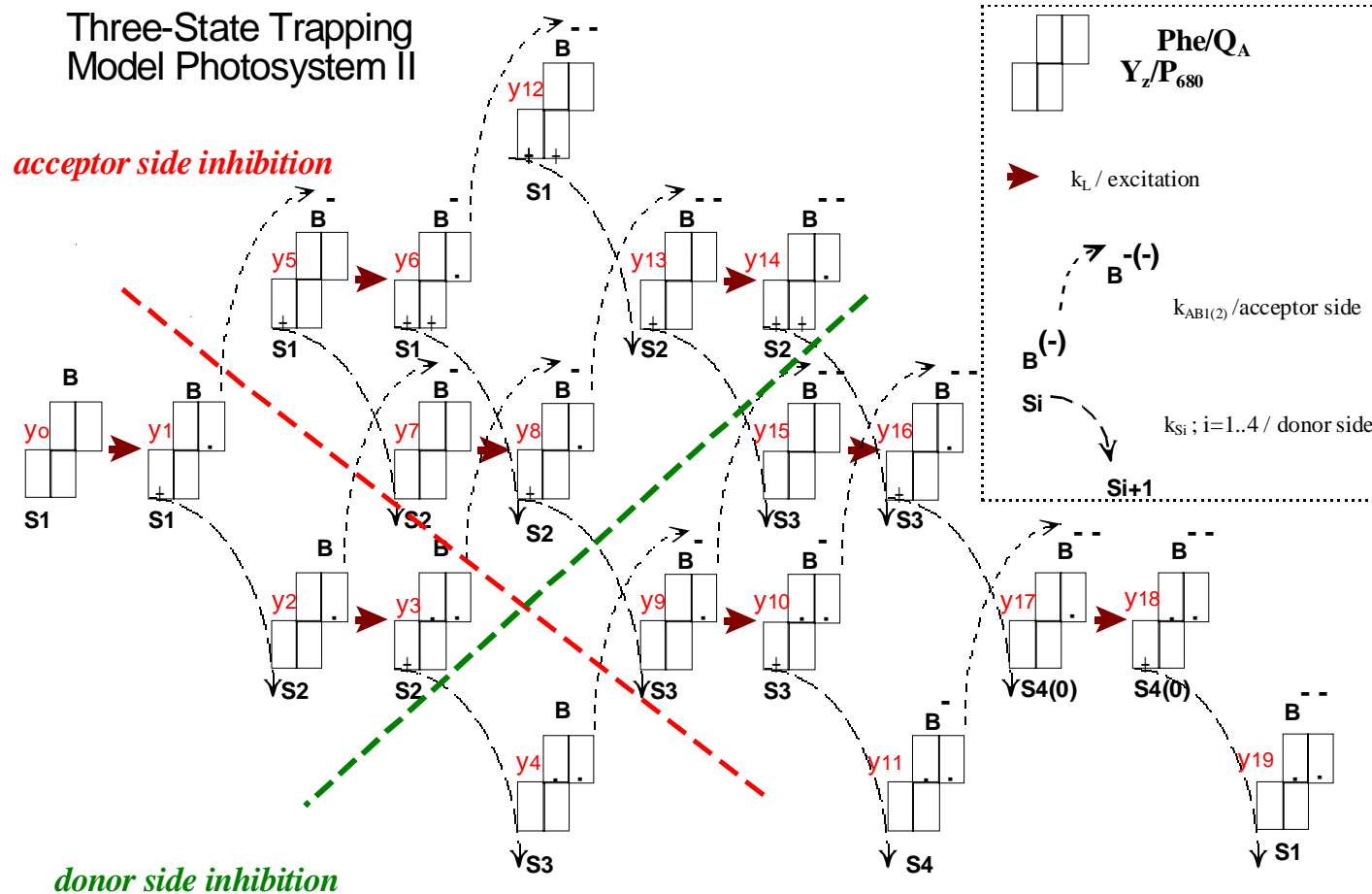


Fig. 1. Model of reaction pattern and $-$ intermediates associated with double-hit requiring RC closure in chloroplasts with OEC in dark-adapted S1 state (y_0 , at left hand side of 3rd row). The vertically stacked box pair represents the primary donor-acceptor pair P_{680} -Phe of the RC; the horizontally attached boxes at the bottom and upper position are the secondary donor (Y_Z) and acceptor (Q_A), respectively. Horizontal arrows mark light excitation with rate constant k_L . Downward pointing arrows mark e-transport from OEC to oxidized secondary donor Y_Z^+ with rate constant k_S determined by the S-state involved; upward directed arrows mark e-transfer to Q_B side (B), with rate constants $k_{AB1(2)}$ (see further insert). Light excitations of states y_1 , y_8 and y_{16} have been omitted because of a high rate of radical pair recombination for these states. The relative variable fluorescence yield for each state in the upper three lines is $rFv=0$; in the 4th line with semi-open (y_2, y_9, y_{17}) or quenched closed states (y_3, y_{10}, y_{17}) $rFv=0.5$ and in the bottom line with closed states $rFv=1$.

Q_A^- and the secondary quinone acceptor ($k_{AB1,2}$) at the donor and acceptor side of PS II, respectively. Transient states associated with charge separation have been omitted because of the high rate of primary electron transfer at donor and acceptor side relative to the time window (10 μ s). The open and closed states of the RC in S_1 are designated with y_0 and y_{19} , respectively. The time function of the relative concentration of each state ($y_i(t)$, $i=0, \dots, 19$) is obtained from the numerical solution of the set of 20 differential equations, one for each state. A similar approach, but based on a fundamentally different trapping model, has been used by others (Lazar et al, 1998, Stirbet et al, 1998). The figure is intended to visualize at each box (state) the corresponding equation. For example:

$$dy_8/dt = k_L * y_7 + k_1 * y_6 + k_{AB1} * y_3 - (k_2 + k_{AB2}) * y_8$$

The numerical solution of the time course of the relative fluorescence yield (rFv) is then obtained by substitution

$rFv(t) = rFv(t, k_L, k_1, k_2, k_3, k_4, k_{AB1}, k_{AB2}) = [y_4 + y_{11} + y_{19}] + 0.5 * [y_2 + y_3 + y_9 + y_{10} + y_{17} + y_{18}]$,
or in an alternative representation

$$F(t) = F(t, k_L, k_1, k_2, k_3, k_4, k_{AB1}, k_{AB2}, \phi_p) = 1 + \phi_p * [rFv(t) - 1],$$

in which for the closed states $rFv(t) = F(t) = 1$ and for the open state, with $rFv(t) = 0$, $F(t) = 1 - \phi_p$ where ϕ_p is the photochemical efficiency of PSII. In the presence of DCMU the reaction pattern for a system with all OEC in S_1 (see fig. 1) is $y_0 \rightarrow y_1 \rightarrow y_2 \rightarrow y_4$ (when $i=1$). The set of 4 ODE's in this case can be solved quantitatively and one obtains a three-exponential function

$$F_i(t) = F(t, k_L, k_i, k_{i+1}) = 1 - \phi_p [\alpha_{iL} \exp(-k_L t) + \alpha_{i1} \exp(-k_i t) + \alpha_{i2} \exp(-k_{i+1} t)]$$

with α_{iL} , α_{i1} and α_{i2} determined by k_L , k_i and k_{i+1} in a known relation. The $F(t) = 1$ level is taken at the maximal fluorescence level measured in the presence of DCMU, which in leaves coincides with the I-level which, as an average, is 10-15% below the P-level. For a dark adapted system with heterogeneity in S-states the expression of the fluorescence induction is

$$F(t) = \sum [\sigma_i * F_i(t)]$$

in which σ_i ($i = 0 \dots 3$) is the fraction of the population in the $S=S_i$ state, $\sum \sigma_i = 1$ and $F_i(t)$ is as defined before.

Fig. 2 shows the experimental and simulated $F(t)$ curve of *Chenopodium* chloroplasts in the absence and presence of DCMU. In agreement with what has been noticed and interpreted by others (Crofts and Wraight 1983; Lazar et al, 1998; Vredenberg, 2000) $F(0)$ in the presence of DCMU is approx. 50% higher than the initial fluorescence level F_0 in the control, whereas F_m is approx. 10% below the maximal fluorescence reached at the P-level in the control (F_p). Furthermore the figure is conclusive with the following characteristics of the fluorescence curve in a 1 s light pulse: i) the half time of the initial fluorescence increase is not inversely related to the light intensity at excitation rates above 5 ms^{-1} ; ii) the sigmoidal fluorescence rise at excitation rates of the order of 1 ms^{-1} converts into an exponential rise upon an increase in the range above $10\text{-}10^2 \text{ ms}^{-1}$, and iii) the rate constant of the fluorescence rise becomes invariable at

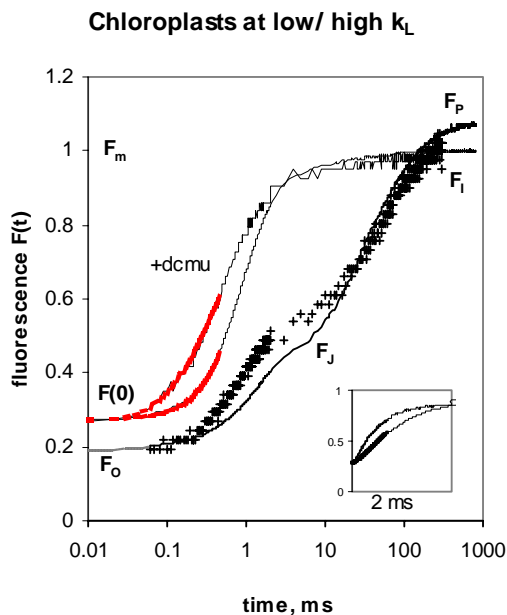


Fig. 2 Fluorescence in 1 s light pulse in *Chenopodium* chloroplasts in absence (right hand set) and presence of 30 μ M DCMU plotted on a logarithmic and linear (insert) time scale. The upper and lower curve in each pair are at a 10-fold different excitation rate with $k_L = 35$ and 3.4 ms^{-1} , respectively. Smooth curves are quantitative fits.

high excitation rates and modulates with the redox state of the oxygen evolving complex (OEC). The likely equivalence of the rate constants k_i (Fig. 1) with those for the oxidation of the OEC in the S_i states (Babcock, 1987) suggests the following approximate k_i -values (in ms^{-1}) for PSII fluorescence in a DCMU-inhibited preparation with proper functioning OEC complex: 30, 10, 3, 0.5 for $i = 0, 1, 2, 3$, respectively. The slow component in the 1-5 ms region of the DCMU-fluorescence curve is presumed to originate from a population in S_3 . There is also experimental indication that this population is identical with the one with semi open centers after DCMU addition. Note that according to the equation above (in bold) the fluorescence induction in the presence of DCMU for a homogeneous population of PSII centers is a three-exponential function. This sets limits to analyses done so far on the DCMU fluorescence induction curve in which an multi-exponential fluorescence curve has been analysed as a sum of mono-exponential functions and interpreted to arise from a population of PSII centers with heterogeneity in antennae size (Melis and Homann, 1975, Govindjee 1995). Current classification of RC's differing in fluorescence properties will require renewed attention and analysis.

Figure 3 shows the experimental and fitted fluorescence induction curve of the upper surface of a *Solanum nigrum* leaf (S-type). The higher k_L is conclusive with a lower chlorophyll concentration in the mesophylls at the (shaded) abaxial leaf surface. This observation is also found in leaves of other plant species. The $F(t)$ curve with donor side inhibition (i.e. $k_2=0$) is also shown. Similarities with experimental curves measured after heat stress are apparent (see for instance Strasser, 1995, Bulychev and Vredenberg, 2001)

In conclusion, the shape and reaction components of the fluorescence induction curve $F(t)$ are of particular interest with respect to current views on PSII heterogeneity, PSII connectivity and activity of the OEC. Analysis of the induction curve in terms of rate constants of light and dark reactions at the donor- and acceptor side of PS II offers a supreme diagnostic tool for localizing and quantifying the effect of stress conditions (UV, drought, heat, and inhibitors) on photosynthetic performance.

References

- Babcock, G.T. (1987), in: *New Comprehensive Biochemistry*, vol 15, Elsevier, Amsterdam,, pp. 125-158.
- Bulychev, A.A. and W.J. Vredenberg (2001), *Bioelectrochemistry*, in press.
- Crofts, A.R. and C.Wraight (1983), *Biochim Biophys Acta* **1409**, 149-185.
- Govindjee (1995), *Austr J Plant Physiol* **22**, 131-160.
- Lazár, D. , M.Brokes, J.Naus, and L.Dvorak (1998), *J Theor Biol* **191**, 79-86.
- Melis, A and P. Homann (1975), *Photochem Photobiol.* **21**, 431-437.
- Stirbet, A.D., Govindjee, B.J. Strasser, and R.J. Strasser (1998), *J Theor Biol* **193**, 131-151.
- Strasser, B.J. (1995) *Photosynthesis Research* **52**, 147-155
- Strasser, R.J., A.Srivastava and Govindjee (1995), *Photochem Photobiol* **61**, 33-42.
- Vredenberg, W.J. (2000), *Biophysical Journal* **79**, 26-38.

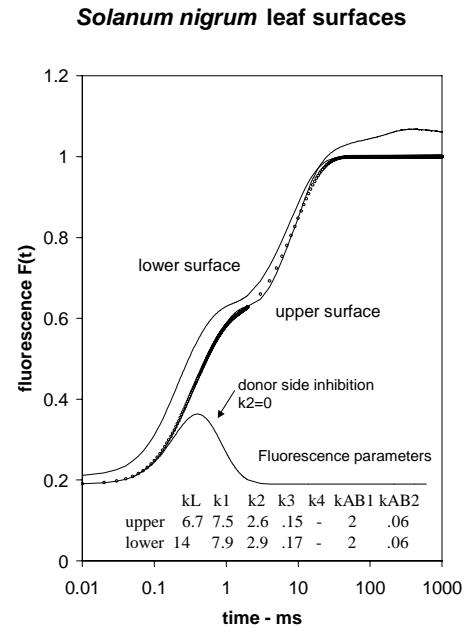


Fig. 3 Fluorescence in 1 s light pulse of upper and lower surface of a *Solanum* leaf, plotted on a logarithmic time scale. The fitted curve (symbols) of the upper surface is shown. Kinetic parameters are given. Note the main difference in k_L . The lowest curve is the simulated $F(t)$ curve under donor side inhibition, i.e. with $k_2=0$.